A frequency-offset estimation algorithm combines code and time features for the remote reception of a weak satellite signal

Renhao Liu & Zhongliang Deng

Published online: 07 Sep 2017.

Submit your article to this journal ☞

Article views: 89

View Crossmark data ☞

Taylor & Francis
Taylor & Francis Group

REGULAR PAPER

⚹ OPEN ACCESS   🔄 Check for updates

A frequency-offset estimation algorithm combines code and time features for the remote reception of a weak satellite signal

Renhao Liu and Zhongliang Deng

School of Electronic Engineering, Beijing University of Posts and Telecommunications, Haidian, China

ABSTRACT

Remote control technology has greatly expanded the intelligence and automation of industry. Satellite signals are important to keep in contact with the facilities and devices in remote areas. However, satellite channels suffer from multi-scale attenuation to achieve reliable communications, which cannot provide sufficient accuracy and suitable complexity for the frequency-offset estimation of a weak signal.

Therefore, this paper focused on a frequency-offset estimation method for a weak signal from a distant, poor satellite channel. First, we built a model of a distant satellite channel with mirror power reflection, considering large fading and multi-path fading simultaneously. Second, we described M-Walsh pilots and a signal vector matrix as they relate to satellite signals. Initially, we analysed the performance of different frequency-offset estimation methods in the satellite environment as opposed to the ground environment. We proposed compact M-Walsh pilots locking correlation to improve the estimation accuracy, which enhanced the frequency tracking. We further proposed equivalent weighting estimation allocation to help improve the balance of accuracy and complexity in the algorithm. Simulations and tests demonstrated that the new algorithm enhanced the root-mean-square-error frequency-offset estimate by 36.2% and the bit-to-error rate) performance by 29.5%.

1. Introduction

Remote control technology has greatly expanded the intelligence and automation of industry, which allows the unattended management of distant and inaccessible facilities and devices [1].

The development of satellite mobile communications, especially Space-Ground Integrated Network (SGIN), has allowed remote control to reach anywhere covered by a satellite signal. Large and complex engineering projects such as dam supervision, the control of substations or farm management can be easily remotely carried out by a person sitting at a monitor in an indoor laboratory.

Satellite signals are important to keep in touch with facilities and devices in the remote areas that are not serviced by a ground communications network. No base station and Wireless Local Area Network exist to transmit control information. A satellite channel is the only way to access such remote areas, ignoring distance and terrain.

However, satellite channels suffer from multi-scale attenuation to achieve reliable communications. The signal power attenuation from a geosynchronous orbiting (GEO) satellite to the ground is approximately 187 dB. A GEO satellite is 35,800 km away from the earth. The focus frequency is 1.55–3.4 GHz. Furthermore, the shadow environment causes signals with serious multi-path fading. The receivers are always moving, which causes a Doppler frequency offset to occur. Therefore, the received signals are always weak. Such systems and communication links are described in Figure 1.

Frequency-offset estimation is important for devices to compensate for demodulation errors from multi-path fading and Doppler frequency offset.

Data-aid and non-data-aid estimation methods are two popular methods for enhancing the accuracy of a frequency-offset estimation. Data-aid estimation methods exploit preamble pilots to make a strong correlation between a local and received signal. The correlation peak indicates the degree of matching between estimated value and the actual frequency offset [2,3]. However, data-aid estimation methods depend on accurate symbol synchronization and have a long delay from the satellite channel that causes a symbol tracking error. Extra preamble pilots also increase the code overhead. A Fourier transform could make signals into the frequency domain. Frequency correlation directly searches for the nearest peak and ignores unaligned symbols [4,5]. Differently, fast Fourier transform increases the computational complexity of the methods in the devices, which require an appropriate balance for optimum estimation. Non-data-aid estimation methods use a correlation calculation
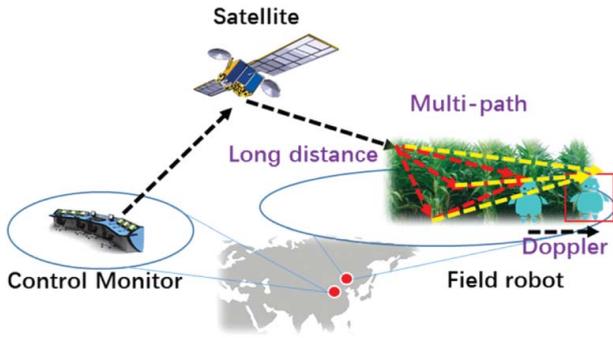

CONTACT   Renhao Liu   ✉ buptlk@bupt.edu.cn

Figure 1. Signal attenuation from a satellite to the ground.

Figure 2. Channel characteristics in satellite environment.

between the received signal and the signal after a phase delay. Primarily, it enlarges the features of the frequency shift, while retaining the same noise background [6,7]. Such methods require much less computing resources than data-aid estimation methods. However, the accuracy of non-data-aid estimation methods degrades when satellite channels weaken.

Above all, this paper focuses on frequency-offset estimation method for a weak signal from a distant and poor satellite channel. First, we built a model of a distant satellite channel with mirror power reflection, considering large fading and multi-path fading simultaneously. Second, we described M-Walsh pilots and a signal vector matrix as they relate to satellite signals. We initially analysed the performance of different frequency-offset estimation methods in the satellite environment as opposed to the ground environment. We proposed a compact M-Walsh pilot locking correlation to improve the estimation accuracy, which enhanced the frequency tracking. We further proposed equivalent weighting estimation allocation to help improve the balance of accuracy and complexity in the algorithm. Simulations and tests demonstrated that the new algorithm enhanced the root-mean-square-error (RMSE) frequency-offset estimate by 36.2% and the bit-to-error rate (BER) performance by 29.5%.

2. The performance of the distant satellite channel model and the frequency-offset methods

2.1. Satellite channels with mirror power reflect

Distant satellite channels consist of two different parts, long-distance attenuation channels and time-variable multi-path fading channels. Long-distance attenuation channels are the links from the satellite to the ground. Time-variable multi-path fading channels are the links associated with devices. Loo [7] proposed a channel model to build referred probability distributions combined shadow fading and multi-path fading. Assume that signal received $r(t)$ is
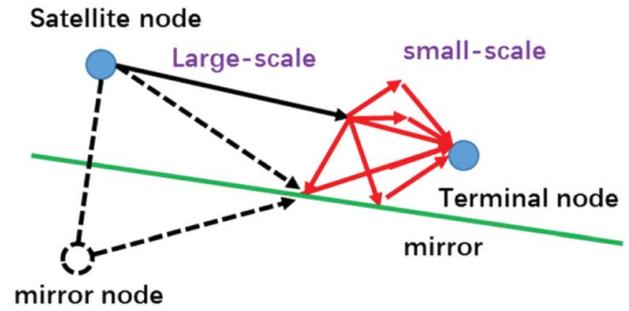
$$r(t) = p(t) + \sum_{i=0}^{L} d(t). \tag{1}$$

Here, $p(t)$ is the direct radiance of the satellite signal, which obeys log-normal distribution yielding

$$P_\rho(\rho) = \frac{1}{\rho s \sqrt{2\pi}} \exp\left[-\frac{\ln(\rho - m_1)^2}{2s^2}\right]. \tag{2}$$

Here, m and s is the mean and variance of lin ρ, and $d(t)$ is the multi-path signal after L ground refractions, which conforms to a Rayleigh distribution with mean of m_2 and is a variant of σ^2. The probability distribution for a multi-path signal is

$$P_d(d) = \frac{1}{d\sigma\sqrt{2\pi}} \exp\left[-\frac{\ln(d - m_2)^2}{2\sigma^2}\right], \quad r \gg \sigma. \tag{3}$$

Satellite signals have large attenuation and obey probability distributions with large-scale fading and small-scale fading simultaneously, as Figure 2 shows.

Actually, the direct radiance of a satellite signal after a long-distance transition would be sufficiently low power. Different paths for small-scale fading can be considered a sum of different direct radiance values after mirroring is assumed, and the received signal $r(t)$ is

$$r(t) = p(t) + \sum_{i=0}^{l} \sum_{i=0}^{L} d(t). \tag{4}$$

Here, l is the number of reflections from each path. We set a mirror threshold of P_{th}, and if the power of the received signals is less than P_{th}, we would only consider large-scale fading. The joint probability distribution can be described as

$$P_r(r) = \frac{\int_{t=0}^{t=r} P_\rho(t)dt + \sum_0^l \int_{t=0}^{t=r} P_d(t)dt}{P_\rho(r)P_d(r)}. \tag{5}$$

2.2. M-Walsh pilots in a signal frame

The channel access method of observed satellite systems is the sat-ground CDMA (satellite to ground Code Division Multi Access) [8]. The signal from an uplink has a permanent frame structure, which
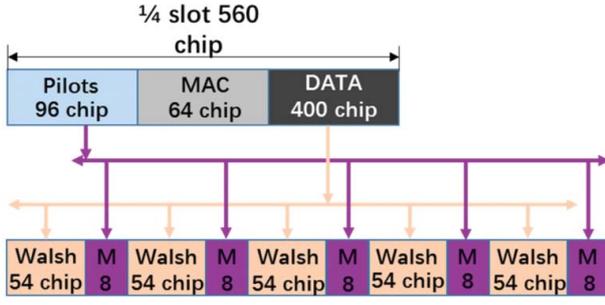
Figure 3. M-Walsh pilots frame structure.

includes pilots, media access control payloads and data payloads, as Figure 3 shows. Walsh symbols have a good cross-correlation performance.

Multi-path fading contributes to much performance degradation with weak randomness from code [9]. Therefore, we designed M-Walsh (M-sequence and Walsh) pilots and a signal vector matrix for the satellite signals as Figure 3 shows.

In our designs, we use alternating Walsh symbols and M-sequence. Walsh functions can provide a complete orthogonal set of symbols. Periodicity and the reproduction of every binary sequence arise from the M-sequence. As a result, M-Walsh pilots have a better auto-correlation performance and strong randomness to compensate for the degradation due to small-scale fading.

As Figure 3 shows, we set five groups of M-Walsh pilots, with one group of Walsh symbols and one group of M-sequence in a single group of M-Walsh. Five groups of Walsh symbols were extracted from 400 chips of data payloads, which carry 54 chips in each group. In addition, the five groups of M-sequence symbols were spread from the pilots with eight chips per group. The M-Walsh pilots provide strong synchronization properties to improve symbol randomness and anti-jamming.

2.3. Performance analysis of different ground frequency-offset estimations in satellite channel

Obvious differences exist between ground channels and satellite channels. Therefore, we analysed the performance of different popular ground frequency-offset estimation methods in the satellite environment. Kay, Fitz and L&R [10] are the ground algorithms considered.

Moreover, we demonstrated a vector matrix for the received signal and the accuracy of each frequency-offset estimation method.

The ith chip in the kth sequence $s_i^{(k)}$ would be sent to a radio. After a receiver receives it, the received signal vector matrix is

$$y_i^{(k)} = c(t) * e^{j2\pi\Delta f(54k+i)T_s+\varphi_0} s_i^{(k)} + \eta \qquad (6)$$

where Δf is the frequency offset in the channel from the satellite to the ground, T_s is period of the chip, φ_0 is the original phase, η is the white Gauss noise in the satellite channel and $c(t)$ is the pulse response from the satellite channel with mirror power control, which obey a $P_r(r)$ probability distribution.

According to the sat-ground CDMA, pilots of the signal frame are recognized by a receiver, which is pre-set to a local register. Cross-correlation occurs between two signals with local original symbols $s_i^{(k)}$ and received symbols $y_i^{(k)}$:

$$z_i^{(k)} = y_i^{(k)} \ s_i^{(k)} = c'^{(t)} * e^{j2\pi\Delta f(54k+i)T_s+\varphi_0} + \eta'. \qquad (7)$$

Here, $c'(t) = c(t)\left[s_i^{(k)}\right]^*, \eta' = \eta\left[s_i^{(k)}\right]^*.$

Merging the common vector terms between the signals and the noise,

$$z(n) = c'(t) * e^{j2\pi\Delta f(54k+i)T_s+\varphi_0+\theta_i^{(k)}} \qquad (8)$$

Conjugate multiplication between $z(n)$ and $z(n-m)$, m is offset parameter. The frequency-offset measured value around m chips can be calculated, and we obtain the angle mean of N frequency-offset measured values:

$$\hat{\Delta f} = \frac{1}{2\pi m T_s} \sum_{n=1}^{N-m} \gamma(n)\arg\{z(n)z^*(n-m)\}. \qquad (9)$$

Here, $\gamma(n)$ is a weighted coefficient of each measured value. Equation (9) is the main estimation process of the Kay algorithm, which is used for satellite channels with mirror power control. Assuming the chip rate is 1.22 mcps, we take a 16-bit quantization sampling, and the accuracy of Kay algorithm is

$$\text{accu1}(\Delta f) = \frac{1 - \frac{1}{1+\exp\left(\int c'(t)dt\right)}}{2\pi m T_s S} = \frac{1.22 * 10^6}{2\pi m * 2^{16}}. \qquad (10)$$

According to Equation (10), as the offset periods m increase, the accuracy of the measured frequency offset decreases, improving the performance. However, reducing the correlation bits causes a contrast of the two sequences and the offset measured feature, which narrows the measured ranges.

An auto-correlation function (ACF) is introduced to produce more strong time correlation features, so we have

$$R(m) = \frac{1}{N-m} \sum_{n=m}^{N-1} z(n)z^*(n-m). \qquad (11)$$

If $R(m)$ is substituted into Equations (8) and (9), the angle mean of N frequency-offset measured

values is

$$\widehat{\Delta f} = \frac{1}{\pi N(N-1)T_s} \sum_{m=1}^{N-1} \arg\{R(m)\} \qquad (12)$$

Taking the average value of the ACFs of $R(m)$, the weak signals with a power lever below the activation tracking minimum would be obviously eliminated. That is the Fitz method, which applies to satellite channels with mirror power control. The accuracy of the Fitz algorithm is

$$\text{accu2}\,(\Delta f) = \frac{1 - \frac{1}{1+\left(\int c'(t)dt\right)^2}}{2\pi m T_s S} = \frac{1.22 * 10^6}{2\pi m * 2^{16}}. \qquad (13)$$

According to Equation (13), noise or signal interference would be reduced by the ACFs, and the accuracy of the frequency-offset estimation would increase for a more obvious correlation peak.

The L&R algorithm further eliminates noise and signal interference by modifying the weighted mean of the ACFs in Equation (11):

$$\frac{1}{N} \sum_{m=1}^{N-1} R(m) = \frac{1}{N} \sum_{m=1}^{N-1} \left(c(t) * e^{j2\pi\Delta f(54k+i)T_s}\right) + \ddot{\eta}. \qquad (14)$$

Assuming that $|(N-1)\Delta f T_s| < 1$, the convergent frequency-offset estimation is calculated by $\frac{\sin\pi(N-1)\Delta f T_s}{\sin\pi\Delta f T_s}$. Substituting Equation (14) into Equation (12), the accuracy of L&R algorithms is

$$\text{accu3}\,(\Delta f) = \frac{1 - \frac{1}{1+\left(\int c'(t)dt\right)^2}}{2\pi(N-1)T_s S} = \frac{1.22 * 10^6}{2\pi m * 2^{16}}. \qquad (15)$$

2.4. Simulation and performance analysis

We built a simulation environment for satellite channels. To further test the performance of the estimation, we simulated different frequency-offset estimation algorithms in MATLAB.

The signal-to-interference noise ratio (SINR) of the received signal was set as −15 to 5 dB. There are 512 chips and 1024 chips of pilots to measure the frequency offset in a satellite channel. The receiver that captures the frequency offset has a locking threshold of 150 Hz [10]. The accuracy of frequency quantification is configured as 12 bits, so the accuracy of phase angle can be quantized lever as 16 bits. All frequency-offset measured values were processed by a Monte Carlo simulation.

Figure 4 shows that the locking probability of frequency-offset measurement algorithms with a normal signal-to-noise ratio (SNR) in a satellite channel are
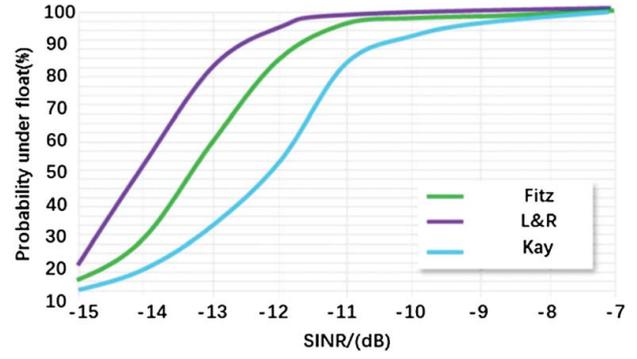

Figure 4. Locking probability of frequency offset under float decimal.

observed by floating and fixed decimal methods. We can determine for an SINR less than −10 dB that the locking probability of the L&R algorithm is better than that of Kay and Fitz. In addition, as the SINR increases, all of them would have a near lever of locking probability because a weighted ACF mean helps an L&R method to eliminate more noise or signal interference.

The locking probability of three frequency-offset algorithms reaches 100% when the SINR is, respectively, −11.6, −10.8 and −8.6 dB for the L&R, Fitz and Kay algorithms. With an SINR of −13.6 dB, the locking probability of L&R is 82.7%, meaning that 17.3% of the transmitted symbols would be lost from frequency-offset estimation alone for possible poor channels.

The correlation peak values for the different algorithms are also shown in Figure 5.

The L&R algorithms have an obvious normalized correlation peak to indicate the correlation between received and local signals that determines the characteristics of the frequency-offset estimations in the chip periods. In contrast, the normalized correlation peaks for the other two methods can be found twice in the chip periods.

Figure 5 shows that the main correlation peak of the Fitz and Kay algorithms are lower than that of the L&R algorithm. However, the next peak is close to the other, which would degrade locking probability of the frequency offset.
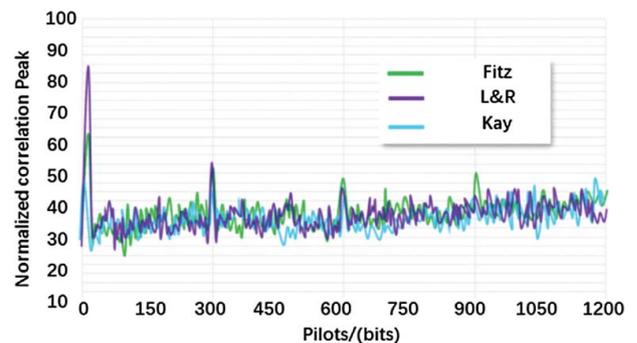

Figure 5. Normalized correlation peak under the float decimal.

3. New frequency-offset estimation method combined with code and time features

Traditional frequency-offset estimation methods suffer from long-distance power attenuation and serious multi-path fading and are limited by low accuracy and a restricted range of the satellite channel. M-Walsh pilots contribute to strong synchronization properties to improve symbol randomness and anti-jamming. Since the transmitter has a new frame structure, a suitable synchronization method including a frequency-offset estimation must be proposed to enhance the performance of the receiver, under the condition of noise and frequency offset.

To improve the estimation accuracy, we propose a new compacted M-Walsh pilots locking correlation, which enhances the frequency tracking. Furthermore, our proposed equivalent weighting estimation allocation can help improve the balance of accuracy and complexity in the algorithm.

3.1. Compacted M-Walsh pilots locking correlation

M-Walsh pilots are characterized by strong correlation and synchronization. In a satellite channel, we must calculate the estimation values by a series of calculations. There are 56 chip Walsh symbols and 8 chip M-sequences in a group of pilots. First, cross-correlations in the Walsh symbols are exploited to obtain the initial frequency-offset estimated values. Next, the M-sequence compensates for the initial frequency-offset estimated values by eliminating the noise. Correlations of the next groups of pilots lock the frequency-offset estimation probability, which also controls the estimation range. The compacted M-Walsh pilots locking correlation is shown in Figure 6.

Received Walsh symbols vector matrix can be described as

$$y\_w_i^{(k)} = c(t) * e^{j2\pi\Delta f(54k+i)T_s+\varphi_0} s_{wi}^{(k)} + \eta. \quad (16)$$

Here, $s\_w_i^{(k)}$ are the Walsh symbol signals, and $i = 54\alpha + \beta$, $0\le\alpha\le4$, $0\le\beta\le53$. First, we focus on
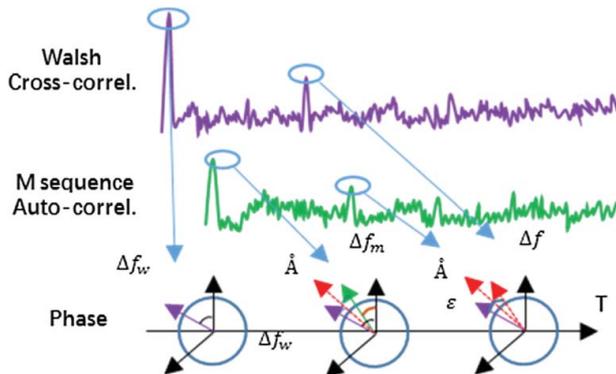

Figure 6. Compacted M-Walsh pilots locking correlation.

one sequence with five block chips of Walsh symbols and M-sequences. $y\_w_i^{(k)}$ is cross-correlated with the local original Walsh symbols:

$$z\_w_i^{(k)} = y\_w_i^{(k)} \quad s\_w_i^{(k)} = c''(t) \ * e^{j2\pi\Delta f(54k+i)T_s+\varphi_0} + \eta'. \quad (17)$$

To obtain the effect of satellite channels with mirror power control, $c''(t)$ is transformed as $s\_w_i^{(k)} c(t)\left[s\_w_i^{(k)}\right]^*$.

As the Walsh symbols are carried as periodic signals, there are finite discontinuous points in a restricted period; signal amplitudes are also restricted and absolutely integral. We used Fourier series of $c''(t)$, which satisfies Dirichlet's distribution [11]:

$$c''(t) = a_0 \ c(t) + \sum_{j=1}^{\infty} a_j c(t)\cos j2\pi\Delta f_w t$$

$$+ \sum_{j=1}^{\infty} b_j c(t)\cos j2\pi\Delta f_w t \quad (18)$$

For the odd function features of the Walsh period signals, the parameters are $a_0 = a_j = 0$, according to a half-period waveform calculation:

$$b_j = \frac{4}{T_s} \int_0^{T_s/2} c''(t)\sin j2\pi\Delta f_w t dt \quad (19)$$

Therefore, $c''(t)$ has sinusoidal harmonic components with the parameters b_j. A half period $[0, \ 1/2T_s]$ contains six discontinuity points [12]. Referring to Parseval's theorem, the sum of the squares of a function is equal to the sum (or integral) of the square of its transform. The six discontinuity points of b_j are 0, $1/j\Delta f_w$, $2/j\Delta f_w$, $3/j\Delta f_w$, $4/j\Delta f_w$ and $5/j\Delta f_w$. Therefore, the power of the $c''(t)$ period can be the sum of squares of each harmonic component, that is,

$$\frac{1}{2}\sum_{j=1}^{\infty} b_j = \frac{1}{T_s}\int_0^{T_s/2} c''(t)^2 dt = \sum_{i=1}^{\infty}\int_0^{T_s/2} P_r(r)dr \ E_s \quad (20)$$

E_s is the power of Walsh chip power. Combining Equations (20), (16) and (9), the frequency offset Δf_w measured by the Walsh symbols would be

$$\Delta f_w = \frac{1}{2\pi m T_s E_s}\sum_{n=1}^{N-m} \arg\{z(n)z^*(n-m)\} \quad (21)$$

To compensate for the error of the initial frequency-offset estimation, an auto-correlation into the M-sequence is attempted. Considering the same block sequence, the first block of the M-sequence has 54 chips after the Walsh chips. Both share the same ability of

time synchronization. The strong randomness of the M-sequence compensates for the degradation from small-scale fading of the estimation. We implement auto-correlation to calculate the ACFs of the M-sequence chips:

$$\frac{1}{N} \sum_{m=1}^{N-1} R(m) = \frac{1}{N-m} \sum_{n=m}^{N-1} z(n)z^*(n-m)$$

$$= \frac{1}{N-m} \sum_{n=m}^{N-1} y_m i^{(k)} s_m i^{(k)}(n) y_m i^{(k)} s_m i^{(k)*}(n-m)$$

$$(22)$$

$s\_m_i^{(k)}$ is the signal of the M-sequence symbols, and $d = 7\alpha + \beta, 0 \le \alpha \le 4, 0 \le \beta \le 7$. When the number of the M-sequence symbols is large enough, the ACFs of M-sequence chips are close to the ACFs of the discrete bits white noise sequence, which has a δ function feature of the ACFs of White Gauss noise. The power spectral density is

$$S_m\ (2\pi\Delta f_m) = \frac{2\pi A^2}{N}\ \delta(2\pi\Delta f_m)$$

$$- \frac{2\pi A^2(N+1)}{N^2} \operatorname{sinc}(2\pi\Delta f_m) \sum_{-\infty}^{\infty} \delta(2\pi\Delta f_m - nw_0).$$

$$(23)$$

The frequency offset Δf_m measured by the Walsh symbols is

$$\Delta f_m = \frac{1}{2\pi N(N-1)T_s} \sum_{m=1}^{N-1} \arg\{R(m)\} \qquad (24)$$

3.2. Equivalent weighting estimation allocation

After the compacted M-Walsh pilots locking correlation, the original frequency-offset measurement Δf_w and Δf_m from the Walsh symbols and the M-sequence closely approximate the actual frequency-offset value. However, a balance of accuracy and complexity in the algorithm must still be investigated further. We would like an equivalent weighting estimation allocation for the two series of frequency-offset measurements.

The equivalent weighting parameter $\mathring{A}$ is designed to harmonize Δf_w and Δf_m in each block of chips. The frequency-offset values are

$$\Delta f = \mathring{A}\Delta f_w + (1 - \mathring{A})\Delta f_m \qquad (25)$$

$\mathring{A} \in [0, 1]$, put Equations (21) and (23) into Equation (25), we have

$$\Delta f = \frac{\mathring{A}}{2\pi m T_s E_s} \sum_{n=1}^{N-m} \arg\{R(m)\}$$

$$+ \frac{(1 - \mathring{A})}{2\pi N(N-1)T_s} \sum_{m=1}^{N-1} \arg\{R(m)\} \qquad (26)$$

In order to calculate the exact frequency offset, the variant gradient of Δf would be calculated as

$$\frac{\partial \operatorname{var}(\Delta f)}{\partial t} = \frac{\partial}{\partial t}\left(\frac{\mathring{A}^2}{4\pi^2 m^2 T_s^2 E_s^2} + \frac{(1 - \mathring{A})^2}{4\pi^2 N^2(N-1)^2 T_s^2}\right)$$

$$(27)$$

Once the extremum points are confirmed, $\mathring{A}^2$ provides the exact weighting percentage with the minimum error from the frequency-offset measurement values. After one equivalent weighting confirmation, five chips of the sequence would show the common ability of noise elimination. An accuracy control factor ε can further compensate for the error after correlation, that is,

$$\varepsilon = \frac{1}{N}\sqrt{\sum_{j=1}^{\infty}\left[\left(\frac{1}{N}\sum_{j=1}^{N}\Delta f_w(j)\right) - \Delta f_w(j)\right]^2} \quad (28)$$

After all, the final frequency-offset measured values would be

$$\Delta f = \mathring{A}\Delta f_w + (1 - \mathring{A})\Delta f_m + \varepsilon \qquad (29)$$

3.3. Accuracy and complexity analyses

The compacted M-Walsh pilots locking correlation enhances frequency tracking. At the same time, the equivalent weighting parameter and the accuracy control factor contribute to noise and interference control. Compared with the performance of the Kay, Fitz and L&R algorithms, the accuracy of proposed algorithms is

$$\operatorname{accu4}(\Delta f) = \frac{1}{4\pi^2 T_s^2 S}\left(\frac{1}{m^2 E_s^2} + \frac{\varepsilon}{N^2(N-1)^2}\right) = \frac{1.22 * 10^6}{2\pi m * 2^{16}}$$

$$(30)$$

which is a more accurate and precise frequency-offset estimation that uses a new ε and E_s^2.

Complexity is also an important target for a frequency-offset estimation method. Complex multiplication and angle transformation are the two main operations in the estimation process. There are $N(N-1)/2m$ complex multiplication operations and $N/2m$ angle transformations for the proposed algorithm, and $N - m$ complex multiplication operations and $N - m$ angle transformations for Kay algorithm. Therefore, the proposed algorithm simplifies the process by limiting the equivalent weighting estimation allocation.

4. Simulation and performance analyses

In order to test the performance of the proposed frequency offset estimation method, a simulation
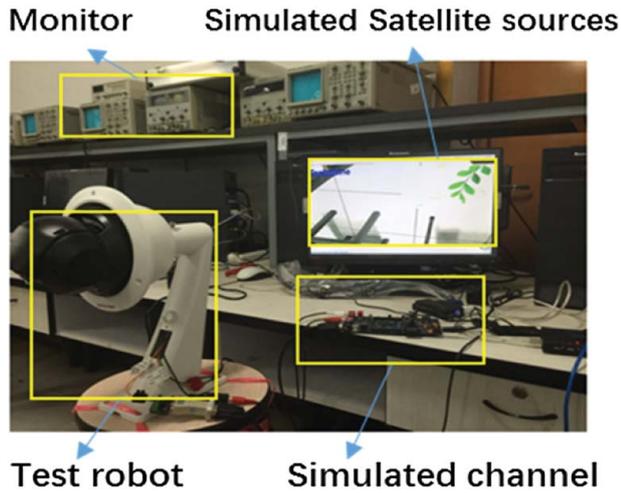
Figure 7. Simulation environment for performance test.

Figure 9. BER performance under frequency-offset estimations.

environment with a hardware platform and software system was built, as shown in Figure 7. Our SGIN remote control environment included a smart terminal on the ground, satellite channels referred to by C. Loo, which is a popular satellite channel model. We used computer software to generate the satellite source signals.

We organized the simulations to produce more accurate results according to Monte Carlo' rules. First, the computer software generated a source signal, which simulated the uplink transmitted signals on the ground. Then, we placed the transmitted signals into an Field-Programmable Gate Array to add channel attenuation. The smart terminal on the ground received the signal from the channel. Before demodulation, signal synchronization adjusted the frequency-offset estimation. We pre-set the frequency offset before the transition. The estimated value was assessed for its closeness to the pre-set values.

The RMSEs of the estimated frequency offset for different SNRs are shown in Figure 8. The BERs of the subsequent decoding were collected and are shown in Figure 9.
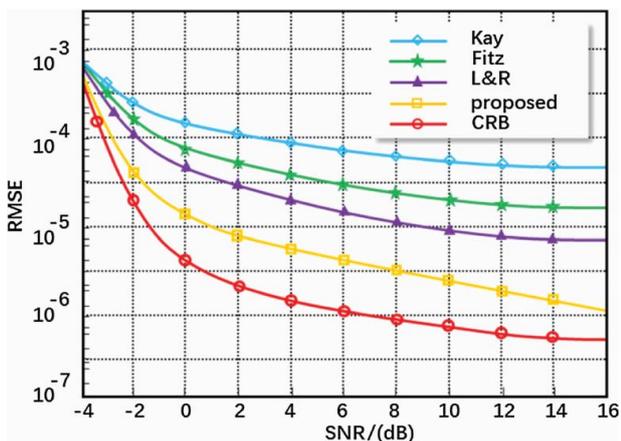
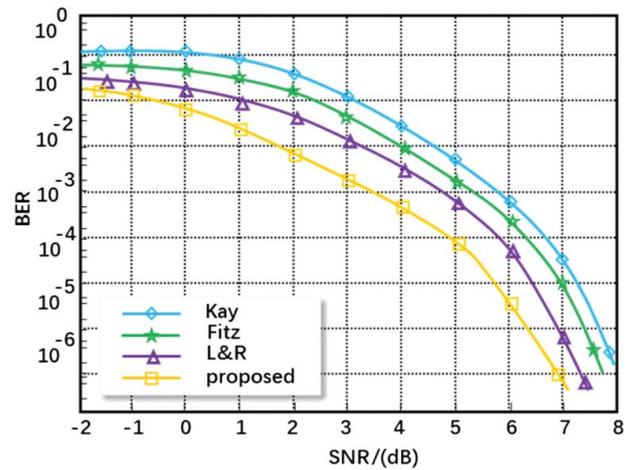Figure 8 shows the RMSEs of the estimated frequency-offset values obtained via four methods with different SNRs. As Figure 8 shows, as the SNR increased, the RMSE of the frequency offset estimation improved for all four methods. A frequency-offset estimation method combining code and time features is much closer to Cramer Rao Bound (CRB) [13]. CRB is a series of minimum estimated values. With the same SNR, the RMSE of the proposed frequency-offset estimation method was lower than for the Kay, Fitz and L&R algorithms.

When the SNR was 6 dB, the RMSE for the proposed frequency-offset measurement was 4.32×10^{-5}, which is approximately 36.2% better than for the L&R algorithms, because the equivalent weighting estimation allocation was improved by noise elimination. Better accuracy was also achieved by unified Walsh symbols and M-sequences.

Figure 9 shows the various BERs after frequency-offset compensation by the four frequency-offset measured methods. With the same SNR, the proposed frequency-offset estimation method gave a better BER. When the SNR was 5 dB, the BER of frequency-offset measurement methods combining the time and code features was 1.27×10^{-4}, which was an approximately 29.5% improvement of the BER. As the SNR increased, the BER improved for all four frequency-offset estimation methods. However, the BER of proposed frequency-offset measured method showed the best performance. It satisfies the condition of a weak signal from the satellite received on the ground. The proposed method combines the code and time to obtain the balance to control noise and interference.

5. Conclusions

A new frequency-offset estimation method combining code and time features for a weak signal from satellite to ground was proposed. A model of a distant satellite channel with mirror power reflection allowed the

Figure 8. RMSE of the estimated frequency offset.

analysis of the characteristics of a remote satellite channel. The frequency-offset estimation method did not show the same performance as those on the ground. The proposed compacted M-Walsh pilots locking correlation enhanced the frequency tracking. An equivalent weighting estimation allocation helped to improve the balance of accuracy and complexity in the algorithm. Simulations and tests demonstrated that the new algorithm enhanced RMSE frequency-offset estimation by 36.2% and the BER by 29.5%.

Disclosure statement

No potential conflict of interest was reported by the authors.

Funding

References

[1] Benedetto F, Giunta G, Bucci S. A unified approach for time-delay estimators spread spectrum communication. IEEE Trans Commun. 2011;59(12):3421–3429.

[2] Gu X, Chang Q, Glennon E, et al. An autonomous satellite time synchronization system using remotely disciplined VC-OCXOs. Sensors. 2015;15:17895–17915.

[3] Gu N, Wu S, Kuang L, et al. Belief propagation-based joint iterative algorithm for detection and decoding in asynchronous CDMA satellite systems. J Wirel Commun Netw. 2013;2013:234.

[4] Zhao J, Zhang X, Zheng B, et al. Design of a search and rescue terminal based on the dual-mode satellite and CDMA network. Sci China Phys Mech Astron. 2010;53(12):2312–2314.

[5] Jan YH. Efficient window-based channel estimation for OFDM system in multi-path fast time-varying channels. IEICE Trans Commun. 2015;E98.B(11):2330–2340.

[6] Beidas B, Seshadri R, Becker N. Multicarrier successive predistortion for nonlinear satellite systems. IEEE Trans Commun. 2015;63(4):1373–1382.

[7] Escrig B, Fares F, Boucheret M, et al. Multi-user detection for the ARGOS satellite system. Int J Satell Commun Netw. 2015;33:1–18.

[8] Ma T, Lee Y, Winkler S, et al. QoS provisioning by power control for video communication via satellite links. Int J Satell Commun Netw. 2015;33:259–275.

[9] Collard F, Gaudenzi R. On the optimum packet power distribution for spread aloha packet detectors with iterative successive interference cancelation. IEEE Trans Wirel Commun. 2014;13(12):6783–6794.

[10] Molisch AF, Tufvesson F. Propagation channel models for next-generation wireless communications systems. IEICE Trans Commun. 2014;E97.B(10):2022–2034.

[11] Deng JH, Feng KT. Time-frequency multiplex estimator design with joint Tx IQ imbalance, CFO, channel estimation, and compensation for multi-carrier systems. IEICE Trans Commun. 2015;E98.B(11):2322–2329.

[12] Li N, Lin W, Shui T, et al. A low-complexity frequency-offset estimation algorithm for the medical body area network. IC-NIDC; Beijing, China. 2012. p. 554–557.

[13] Lin W, Deng ZL. Dimensional functional differential convergence for Cramer-Rao lower bound. J Differ Equa Appl. 2017;23(1-2):249–257.